Space Sci Rev
DOI 10.1007/s11214-017-0332-1

Magnetic Field Perturbations from Currents in the Dark Polar Regions During Quiet Geomagnetic Conditions

E. Friis-Christensen[1] · C.C. Finlay[2] · M. Hesse[3] · K.M. Laundal[3]

Received: 23 March 2016 / Accepted: 17 January 2017

Abstract In the day-side sunlit polar ionosphere the varying and IMF dependent convection creates strong ionospheric currents even during quiet geomagnetic conditions. Observations during such times are often excluded when using satellite data to model the internal geomagnetic main field. Observations from the night-side or local winter during quiet conditions are, however, also influenced by variations in the IMF. In this paper we briefly review the large scale features of the ionospheric currents in the polar regions with emphasis on the current distribution during undisturbed conditions. We examine the distribution of scalar measurements of the magnetic field intensity minus predictions from a geomagnetic field model. These 'residuals' fall into two main categories. One category is consistently distributed according to the well-known ionospheric plasma convection and its associated Birkeland currents. The other category represent contributions caused by geomagnetic activity related to the substorm current wedge around local magnetic midnight. A new observation is a strong IMF B_y control of the residuals in the midnight sector indicating larger ionospheric currents in the substorm current wedge in the northern polar region for $B_y > 0$ and correspondingly in the southern hemisphere for $B_y < 0$.

Keywords IMF · Polar cap · Ionospheric currents · Substorms · Quiet time

1 Introduction

The dedicated satellite missions that have monitored the geomagnetic field during the last nearly two decades, Ørsted, CHAMP and *Swarm*, have been crucial for producing the geomagnetic reference field models that are used extensively in research and applications. The

E. Friis-Christensen, Retired

✉ E. Friis-Christensen
efc@friis-chr.dk

1 Danish National Space Institute, Lyngby, Denmark

2 DTU Space, Lyngby, Denmark

3 University of Bergen, Bergen, Norway

Published online: 02 February 2017

Swarm mission with its improved instrumentation (e.g., Friis-Christensen et al. 2006) and its carefully designed constellation of three satellites promises a significant improvement in our knowledge of the main magnetic field and its temporal variation. The measurements are now so accurate that even data selected during magnetically quiet times do show large systematic deviations (residuals) from the best models at high geomagnetic latitudes during dark conditions. Although the residuals are often characterised as noise, it is important to examine whether this "noise" is systematic and therefore might influence the models of the main field, in particular the models of the lithospheric field and the secular variation of the core field that require high accuracy.

The current systems at high latitudes consist of ionospheric currents connected to the magnetosphere by Birkeland currents along the magnetic field-lines. The magnetic field perturbations from the field-aligned currents, which are perpendicular to the magnetic field lines, contribute only little to the observed scalar magnetic field, which is used for main field modelling at high magnetic latitudes. The ionospheric current systems fall into two main categories: One is part of the substorm current wedge connecting the closed field-line part of the magnetotail with the polar ionosphere via the magnetic field lines to the midnight auroral oval in the ionosphere. The other component of high-latitude ionospheric currents is associated with the always existing, and always varying plasma convection caused by the interaction between the solar wind and the Earth's magnetic field.

In order to obtain the best models describing the main field, i.e. the core field and the lithospheric field, it is important to minimise the influence of the contribution from external fields, in particular the magnetospheric and ionospheric currents. This can be done partly by modelling the known sources and partly by careful selection of the observations that constitute the input data for the modelling. This selection aims at avoiding data during so-called geomagnetically disturbed periods. These include the magnetospheric substorms that are reflected in geomagnetic indices like the *AE* and *Kp* (see, for example Kauristie et al. (2016)). These indices may be used to avoid relatively large and extended substorms, but the poor spatial resolution of the ground based observatory network on which these indices are based may easily imply missing the isolated substorms that often take place during geomagnetically quiet conditions. The occurrence rate as well as the magnitude of substorms depends on the energy that is transferred to the magnetosphere through the interaction between the solar wind and the magnetosphere, in particular through the so-called merging process at the day side. The result of this process is directly observed in the ionospheric convection, which is associated with horizontal ionospheric currents that contribute to the observed high latitude magnetic field. The magnitude of the currents depends both on the convection electric field and on the ionospheric conductivity. This part can therefore be reduced by selecting data corresponding to a small merging electric field in the solar wind and by using data taken during low ionospheric conductivity i.e. dark conditions with limited solar EUV radiation. On the night-side, especially during quiet times, enhanced convection can proceed without substorms, but is still temporally decoupled from the day-side driver such that the merging electric field will not predict well any night-side enhancements.

Ritter et al. (2004) carried out a comprehensive study of the residuals between the scalar field measurements and a high degree field model during the first years of CHAMP. They specifically examined the ionospheric and field-aligned currents during quiet conditions, which they defined by a small root-mean-square (rms) value of the residuals along the satellite orbit in order to identify the prevailing physical conditions for optimising the data selection criteria for geomagnetic main field modelling.

After examining various and commonly used geomagnetic indices Ritter et al. (2004) conclude that there is no single index that is able to identify reliably quiet periods at high

latitude. Apart from the obvious dark ionosphere and northward IMF conditions the most predictive parameter in the solar wind is the merging electric field E_m as defined by Kan and Lee (1979) and Newell et al. (2007). This is expected because a strong merging electric field means increased build-up of magnetic flux in the magnetosphere, which in turn increases instability in the tail and hence the probability of substorm activity. Ritter et al. (2004) find that there is a small difference in the average B_y for quiet conditions in the Northern and Southern Hemisphere winters consistent with a reported, but not explained, stronger westward electrojet for IMF $B_y > 0$ in the Northern Hemisphere during winter months (Friis-Christensen and Wilhjelm 1975).

In this study we examine the residuals of the combined CHAMP and *Swarm* dataset from 2000 to 2014 used in developing the CHAOS-4 and CHAOS-5 geomagnetic field models (Olsen et al. 2014; Finlay et al. 2015). Our main focus is to examine to which degree the relatively well described and understood ionospheric current systems may contribute to the observed residuals relative to the main field model. In particular, we want to examine whether the strong control of the B_y component of the interplanetary magnetic field (IMF) on the plasma convection in the polar regions can be observed in the spatial distribution of the residuals and we want to examine and understand the reported B_y effect on the electrojets in the winter hemispheres.

2 IMF Control of Ionospheric Currents

The currents in the polar ionosphere fall into two main categories. One category is related to the plasma convection from day to night and its associated electric field. This system relatively early got its name the DP2 current system to distinguish this system from the current system associated with the auroral substorm, the DP1 system in the midnight sector. The important role of the interplanetary magnetic field B_z component in the coupling processes between the solar wind and the ionosphere was one of the first issues to be investigated when magnetic field measurements in the solar wind became available (Nishida and Maezawa 1971). The effect of merging between two oppositely directed magnetic fields had already been predicted by Dungey (1961) and observations confirmed that the auroral latitude currents are generally small when the Earth's magnetic field and the IMF are parallel, namely during northward IMF.

In the polar cap, however, poleward of ionospheric currents in the auroral zone, magnetic observatory data showed strong ionospheric currents in the day side and solar illuminated polar cap. This feature was extensively studied by Friis-Christensen et al. (1972) who concluded that a particular component of the IMF, the azimuthal component, B_y, was crucial for this effect. This study was followed by the first identification of the patterns of equivalent current systems at high latitudes that were associated with various IMF orientations (Friis-Christensen and Wilhjelm 1975). In these patterns a new equivalent current system in the day side ionosphere located at higher latitudes than the well-studied auroral zone was identified and coined the "DPY-current". The study was based on limited data from available magnetic observatories in the northern hemisphere. In 1972 a dense magnetometer array was established along the west coast of Greenland poleward of the auroral zone magnetic observatories. This allowed Wilhjelm et al. (1978) to demonstrate that the DPY-current is an ionospheric Hall current sandwiched between two oppositely directed field-aligned current systems simultaneously measured by satellites.

Crooker (1979) developed the concept of antiparallel merging for various IMF orientations and Reiff and Burch (1985) used this concept to formulate a general convection model

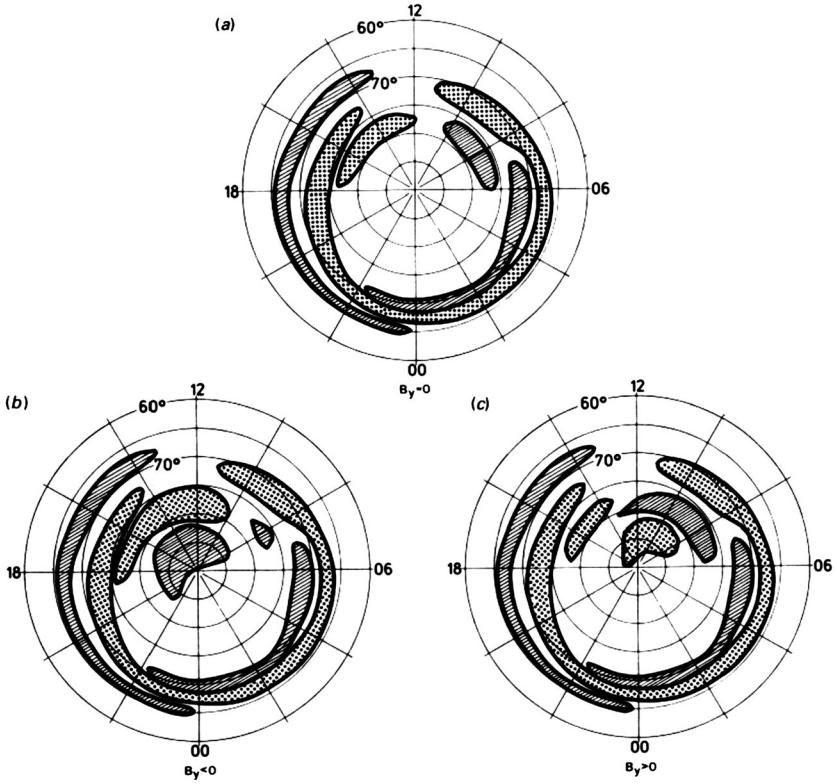

Fig. 1 Model distribution of Birkeland currents on the basis of the statistical distribution obtained by satellite observations and derived from ground-based observations of magnetic fields and aurora. *Hatched areas* indicate downward currents and *dotted areas* upward currents. In (**a**) is shown the distribution for IMF $B_y = 0$ and $B_z = 0$; (**b**) is for $B_y < 0$ and (**c**) is for $B_y > 0$. (Friis-Christensen and Lassen 1991)

for arbitrary orientation of the IMF. The dense magnetometer chain in Greenland, the first of its kind at such high latitudes provided the observations that resulted in the first maps of the complete set of ionospheric currents, field-aligned currents and electric fields for various orientations of the IMF (Friis-Christensen et al. 1985). Using realistic conductivity models for the summer ionosphere they were able to calculate the distribution of field-aligned currents for IMF $B_y > 0$ and $B_y < 0$ demonstrating the dominant pair of oppositely directed Birkeland currents at magnetic local noon with upward currents in the polar cap for $B_y > 0$ and downward currents for $B_y < 0$. Combining patterns of ground-based observations of magnetic perturbations and aurora Friis-Christensen and Lassen (1991) proposed a conceptual model of the distribution of Birkeland currents in the polar cap and auroral oval illustrated in Fig. 1. Both the distribution of discrete aurora and the region 1 Birkeland currents seem to consist of two populations, one in the day-side (region 1a) and one mainly located in the night-side (region 1b). The region 1a part gets particularly intense for northward B_z and is strongly controlled by B_y while the region 1b part becomes stronger when B_z gets more negative and is not supposed to be much affected by B_y.

For small B_y and $B_z > 0$ a small double-cell current system corresponding to reversed convection is observed in the polar cap, separate from the morning and afternoon region 1 current systems. This system, coined the NBZ current (Northward B_z) was discovered by

Iijima et al. (1984) using satellite measurements of the field-aligned currents. The direct measurements proved that the NBZ system was a real and independent current system and not just a statistical phenomenon resulting from averaging of the B_y positive and B_y negative current systems near noon.

Merging on the open magnetic field lines in the tail lobes as discussed in a model presented by Burch et al. (1985) does not involve any magnetic flux being transferred from the day-side to the night-side. Merging between the IMF and day-side closed field lines, on the other hand, implies pile-up of flux in the night-side and subsequent reconnection of these open field lines at some later time. This is the basis for the Expanding-Contracting Polar Cap (EPCP) paradigm of solar wind-magnetosphere-ionosphere coupling (Cowley and Lockwood 1992). Although the physical processes related to the day-side merging and the night-side reconnection are independent, they are of course interrelated through the history of the IMF and the solar-terrestrial coupling. Consistent with the EPCP paradigm Milan (2013) modelled the region 1 and 2 Birkeland current system intensities for varying day-side merging and night-side magnetic reconnection rates and find results consistent with many of the satellite and ground-based observations of magnetic and electric fields and plasmas. The time-dependence between the day-side and night-side processes is a likely source of residual that cannot be modelled by using parameters like the merging electric field.

3 Data Sources

The primary data used in this article are scalar measurements of the magnetic field intensity minus predictions from a geomagnetic field model. We consider only such 'residuals' of data that were actually used in the construction of a field model. These 'residuals' correspond physically to the ground perturbation field, which is typically more simply derived by subtracting an average, or "quiet time value" from the measured field. The majority of the presented examples come from the data set used to construct the CHAOS-5l geomagnetic field model (Finlay et al. 2015). CHAOS-5l estimates the large-scale, time-dependent internal field (to spherical harmonic degree 20), the static lithospheric field (to degree 80) and the large-scale external (magnetospheric) field in SM and GSM coordinates. Further details of the development of the CHAOS model may be found in Olsen et al. (2006) and Olsen et al. (2014).

CHAOS-5l used only data from dark regions (sun at least 10° below the horizon), and in the polar regions relevant here, only scalar intensity data were used. The data were sampled at 60 second intervals. Furthermore, in an attempt to exclude very disturbed conditions, data were only selected when the RC-index (Olsen et al. 2014) changed by at most 2 nT/hr, and when the mean value of E_m over the preceding one hour was less than or equal to 0.8 mV/m, where $E_m = v^{4/3} B_t^{2/3} \sin^{8/3}(|\Theta|/2)$ (Newell et al. 2007) with v the solar wind speed, $B_t = \sqrt{B_y^2 + B_z^2}$ the magnitude of the Interplanetary Magnetic Field (*IMF*) in the y–z plane in *Geocentric Solar Magnetospheric (GSM)* coordinates and $\Theta = \arctan(B_y/B_z)$. Values of the *IMF* and v at five minute resolution were taken from the OMNI database.[1] In all, in the polar regions above 55 degrees quasi-dipole latitude, 121,293 Ørsted scalar data (between March 1999 and June 2013), 188,015 CHAMP scalar data (between August 2000 and September 2010), 26,118 SAC-C scalar data (between January 2001 and December 2004) and 17,485, 17,774, and 16,697 scalar data respectively from the *Swarm Alpha*, *Bravo*

[1] ftp://spdf.gsfc.nasa.gov/pub/data/omni/high_res_omni/

and *Charlie* satellites (between November 2013 and September 2014, release 0302 where available or else 0301) were used. The numbers above refer to individual data points, which were assumed to be independent. In the data selection for the CHAOS-5l model, considering scalar data at polar latitudes, which were used in this study, there is naturally a bias to positive IMF B_z conditions. This bias amounts to 313333 scalar data (81 %) for $B_z > 0$ and 74019 data (19 %) for $B_z < 0$. Below we focus on CHAMP residuals; due to CHAMP's lower altitude, these most clearly show the magnetic disturbances due to polar ionospheric currents.

In addition to scalar residuals from CHAOS-5l, we also present an example from the CHAOS-4h model (Olsen et al. 2014). CHAOS-4h is the high-degree (lithospheric) part of the CHAOS-4 model. The maximum spherical harmonic degree of the static internal part of this model was set to 100. CHAOS-4h was derived only from CHAMP data obtained between September 2008 and September 2010, using a shorter data sampling interval of 30 seconds. The data selection criteria was similar to that for CHAOS-5, except that instead of considering the mean value of E_m in the preceding hour, it used a weighted sum of E_m over the preceding 2 hours (corresponding to the preceding 24 five-minute values) with weights $w_k = \exp(-k\Delta t/0.75\ \text{h})/\sum w_k$. 147,247 scalar data were use to construct CHAOS-4h. A very similar dataset, but including all three vector field components has been used by Kother et al. (2015) for high resolution lithospheric field studies.

4 Ground Magnetometer Activity During Large Residuals

In order to examine the detailed distribution of the observed residuals it is necessary to first understand the origin of the very large residuals since they are most probably related to non-steady state conditions in the ionospheric convection most obviously experienced in connection with substorms. A search for the largest residuals was performed and in order to illustrate the location of those, selected samples including the maximum residual were plotted in a polar diagram. A substorm, small or big, corresponds to an unloading of energy that has been loaded into the magnetosphere by the merging process on the day-side. The substorm events vary in frequency and magnitude. For the relatively small manifestations that we are dealing with in this context, we are further limited in our understanding of these phenomena. That is because the spatial resolution of the ground observatory network is rather poor, in particular in some crucial regions. It is therefore not always possible to identify the cause of the events. However, when looking at the history of the solar wind and in particular the IMF B_y and B_z time variations prior to large residual events we usually observe relatively large time variations. Looking at the merging electric field E_m, which is a function of the B_y and B_z components as well as the solar wind velocity v, we may expect that if the merging field has been large within the previous hour there is a great risk of a disturbance in form of a small substorm. This is illustrated in Fig. 2 showing a large residual due to a substorm occurring about half an hour after a large merging electric field of around 5 mV m^{-1}. This residual originates from the CHAOS-4h dataset that was less strict regarding avoiding periods of large merging electric field as described in Sect. 3. The observation of the enhanced residuals takes place near dawn, in an area without ground based observations. The two SuperMAG plots in Fig. 2 illustrate the development of a substorm in the midnight sector. The first plot suggests that it starts with a strong upward field-aligned current filament (downward precipitating electrons) corresponding to outward radiating equivalent currents consistent with the anticlockwise magnetic field line surrounding the upward field-aligned current. Due to the initial small ionospheric conductivity we do not see any effect of Pedersen currents, which would be oppositely directed. In the next frame the conductivity in the

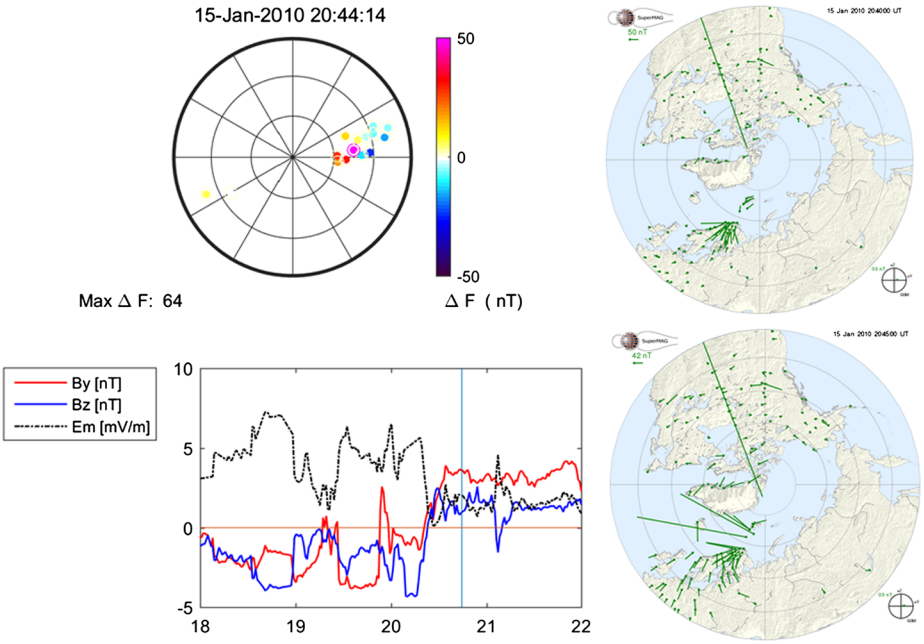

Fig. 2 The *upper left panel* shows a polar plot above 60 degrees quasi-dipole latitude with magnetic local noon at the top. Plotted is a time sequence of residuals observed from CHAMP and colour coded according the magnitude of the residual ΔF. The maximum residual in the sequence is indicated with an extra circle and corresponds to the time indicated at the top of the plot. In the *bottom panel* is plotted time series of IMF B_y, B_z, and the merging electric field E_m before and after the time of the maximum residual indicated by the *vertical light blue line*. On the right-hand side is presented corresponding SuperMAG ground-based magnetometer plots (Gjerloev 2009, 2012) of equivalent currents (*green arrows* are horizontal magnetic field disturbance rotated by 90 degrees). The presented plots are at 20:40 (*top*) and 20:45 (*bottom*)

region has increased and therefore the contribution from the field-aligned currents and the Pedersen currents partly cancel (Fukushima 1976) and we see mainly the development of a westward equivalent current, which we interpret as the westward Hall electrojet. We conclude that the current extends into the dawn sector and that it is the magnetic effect from this current, which is observed in the scalar field on CHAMP, positive (downward) on the poleward side, negative (upward) on the equatorward side. The current is part of the substorm current wedge near midnight, which constitutes the DP1 ionospheric current system.

The magnetosphere is never completely quiet because it constantly has to adapt to the changing solar wind. Whereas the day-side large-scale convection responds in a continuous way to the varying solar wind, the reconnection on the night-side occurs in form of bursts accompanied by particle precipitation, which creates aurora. Some of these develop into substorms that encompass the whole night-side and some only create geographically localised perturbations in the magnetic field. Such an event is seen in Fig. 3. We notice that it occurs during a small merging electric field but we also notice that during several hours prior to the event B_z has been negative, thereby favouring magnetic flux to be transferred from the day to the night-side, which eventually has to be unloaded.

Another kind of magnetic disturbance creating large residuals is related to sudden changes in the orientation of the IMF. An example of this is seen in Fig. 4. Here the *Swarm* satellites are crossing the midnight auroral oval just as a sudden and relatively large change

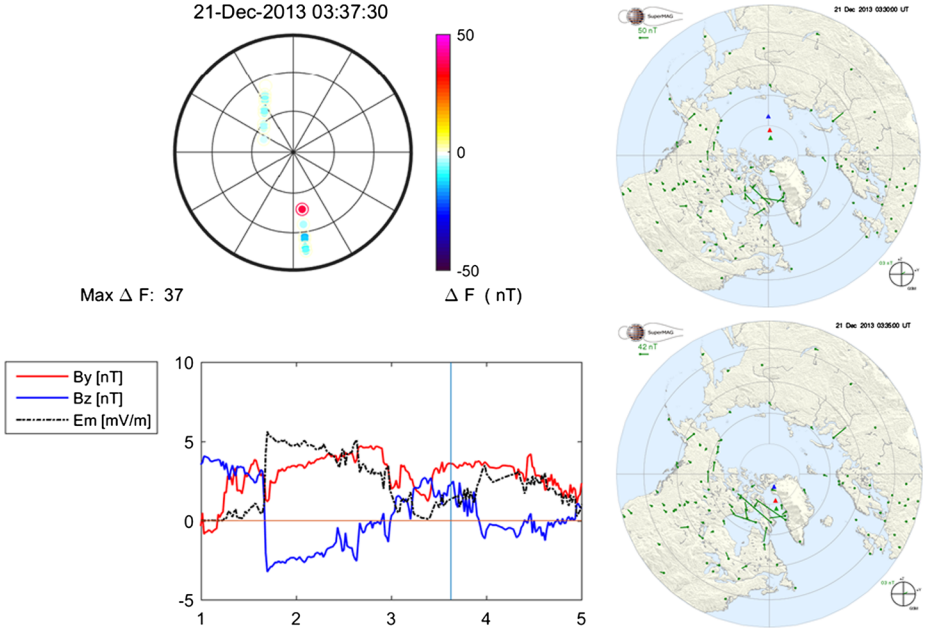

Fig. 3 The *upper left panel* shows a polar plot above 60 degrees quasi-dipole latitude with magnetic local noon at the top. Plotted is a time sequence of residuals observed from *Swarm* and colour coded according the magnitude of the residual ΔF. The maximum residual in the sequence is indicated with an extra circle and corresponds to the time indicated at the top of the plot. In the *bottom panel* is plotted time series of IMF B_y, B_z, and the merging electric field E_m before and after the time of the maximum residual indicated by the *vertical light blue line*. On the right-hand side is presented corresponding SuperMAG ground-based magnetometer plots (Gjerloev 2009, 2012) of equivalent currents (*green arrows* are horizontal magnetic field disturbance rotated by 90 degrees). The presented plots are at 03:30 (*top*) and 03:35 (*bottom*). Footprints of the *Swarm* satellites are shown as *small coloured triangles*

in the B_z and B_y takes place. Apparently the maximum residual is observed a little prior to the IMF change. But although the solar wind data from the OMNI database (see Sect. 3) have been projected to the bow shock we must take into account that there is some uncertainty associated with the projected time of the arrival of the solar wind structure, in particular when there is a major change in the IMF orientation. Whether the satellite observes a magnetic perturbation directly due to the sudden increase in the merging electric field or whether the sudden change in the IMF orientation triggers the start of a substorm is difficult to conclude from the available data but in the latter case the substorm is very short-lived and localised.

5 IMF Control of Observed Residuals in the Day-Side

During substorm-free periods we expect the observed residuals to be controlled by the plasma convection in the polar ionosphere. Therefore, and due to the strong ionospheric currents during day time, main field modelling is often based on observations made in darkness. From ground based magnetic observations it is very difficult to see the B_y related cusp currents around magnetic noon at quiet intervals during the local winter season. One would therefore not expect a large systematic contribution to the observed residuals from ionospheric sources, except during substorm related enhanced precipitation of particles that

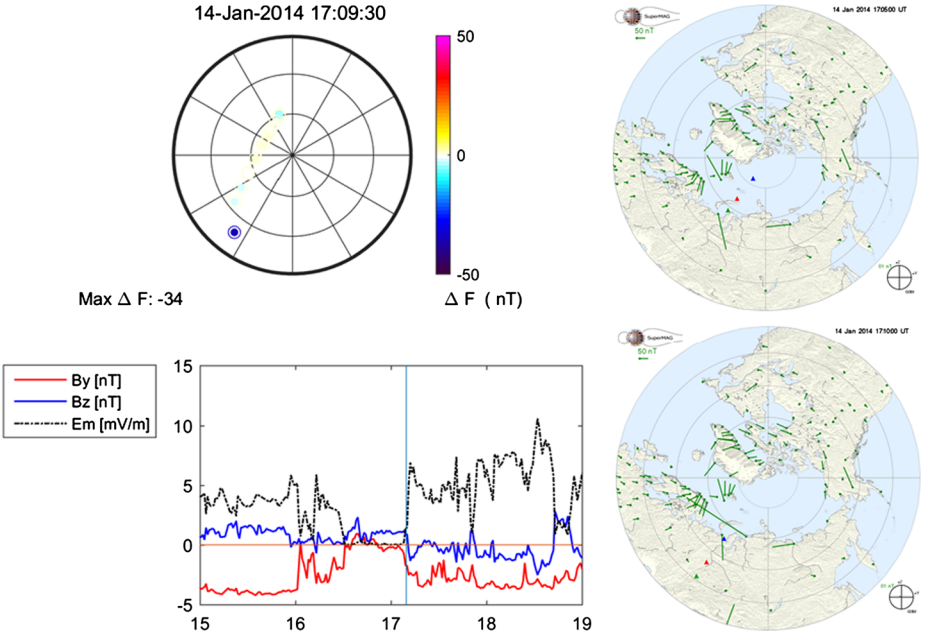

Fig. 4 The *upper left panel* shows a polar plot above 60 degrees quasi-dipole latitude with magnetic local noon at the top. Plotted is a time sequence of residuals observed from *Swarm* and colour coded according the magnitude of the residual ΔF. The maximum residual in the sequence is indicated with an extra circle and corresponds to the time indicated at the top of the plot. In the *bottom panel* is plotted time series of IMF B_y, B_z, and the merging electric field E_m before and after the time of the maximum residual indicated by the *vertical light blue line*. On the right-hand side is presented corresponding SuperMAG ground-based magnetometer plots (Gjerloev 2009, 2012) of equivalent currents (*green arrows* are horizontal magnetic field disturbance rotated by 90 degrees). The presented plots are at 17:05 (*top*) and 17:10 (*bottom*). Footprints of the *Swarm* satellites are shown as *small coloured triangles*

increases the ionospheric conductivity and hence the magnitude of the contribution from ionospheric currents. The number of such events are aimed at being minimised as much as possible taking into consideration the necessity of having a sufficiently large and spatially well distributed data set available for the modelling exercise. As seen in the mass plot of residuals presented by Finlay et al. (2016), there is a systematic distribution of the residuals corresponding to the gross pattern of the auroral zone currents, which means that there must be a sufficient conductivity available in the auroral zone for creating ionospheric currents that can be observed at satellite altitude also during quiet conditions.

To examine to which degree the statistical and well understood convection patterns can be observed in the residuals we have sorted all the residuals according to B_y and B_z but with some additional constraints to avoid contributions arising from changes in the IMF orientations. The IMF values used in the selection correspond to the time when the solar wind reached the bow shock at the front of the magnetosphere. The observed time lag before a change in the IMF is observed in the ionosphere has been measured to be typically around 10 minutes. The necessary time to reconfigure the magnetosphere after a change is typically another 15 minutes (Ridley et al. 1998); therefore, in order to interpret the sign of B_y and B_z correctly we demand that all one minute samples during the previous 30 minutes fulfils the given selection criteria. In this way we decimate the available data but with the combined CHAMP and *Swarm* dataset over a decade or more, we end up with a quite striking result

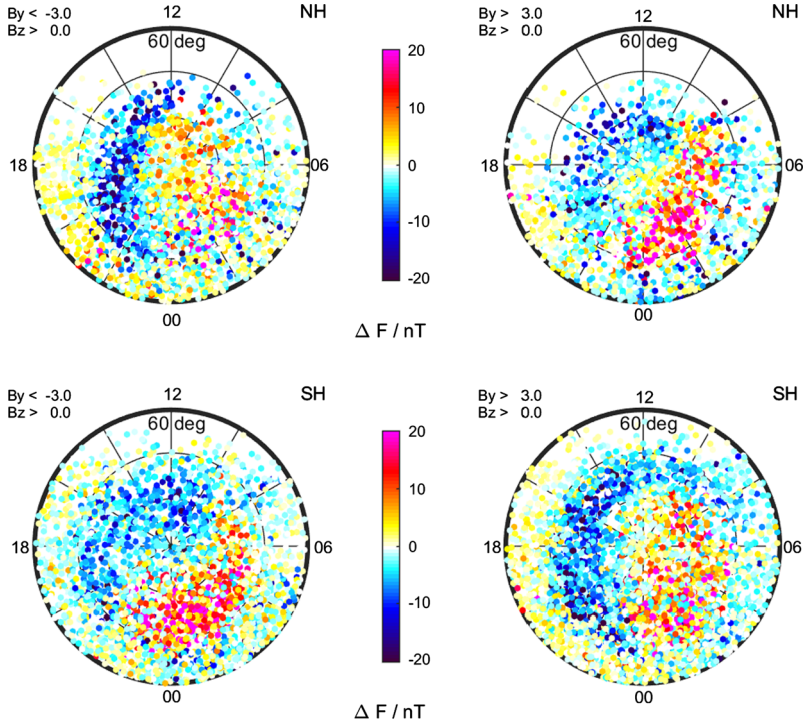

Fig. 5 Polar plot of scalar field residuals from CHAMP and *Swarm* data used to construct the CHAOS-5 model, collected in the northern (*top*) and southern polar region (*bottom*) for $B_y < -3$ nT (*left*) and $B_y > 3$ nT (*right*). Displayed are residuals as a function of QD latitude and magnetic local time. Each *dot* represents a single observation, no binning or averaging has been performed. The scale of ± 20 nT is saturated. The *black circles* delimit QD latitudes of 60, 70 and 80 degrees

in Fig. 5, which shows the distribution according to B_y positive and B_y negative for both hemispheres. The distributions of the residuals are consistent with the statistical patterns derived from the ground based magnetometer and radar measurements and the conceptual models derived from those patterns. There is a high degree of internal consistency meaning a relatively small scatter of the residuals in each local time sector. In the polar cap the ionospheric conductivity is too low to carry substantial currents. The equivalent currents seen from ground-based magnetometers during darkness are therefore predominantly due to the magnetic field from the Birkeland currents, mainly the region 1 currents on the poleward side of the auroral oval (Laundal et al. 2015, 2016). We here interpret the scalar residuals as resulting from the magnetic contribution from the divergence-free part of the total horizontal current system. For a westward horizontal current in the northern hemisphere the magnetic perturbation on the poleward side of the current at satellite altitude is downward, which is in the same direction as the main magnetic field and therefore represents a positive contribution to the scalar field. This is clearly seen by the dominance of positive residuals poleward of the westward electrojet in the morning sector. For the southern hemisphere a westward current produces an upward perturbation on the poleward side, which is also a positive residual. Due to selection criteria the residuals correspond to positive IMF B_z. Therefore, the main distinction between the distribution of the residuals reflects the effect of the IMF

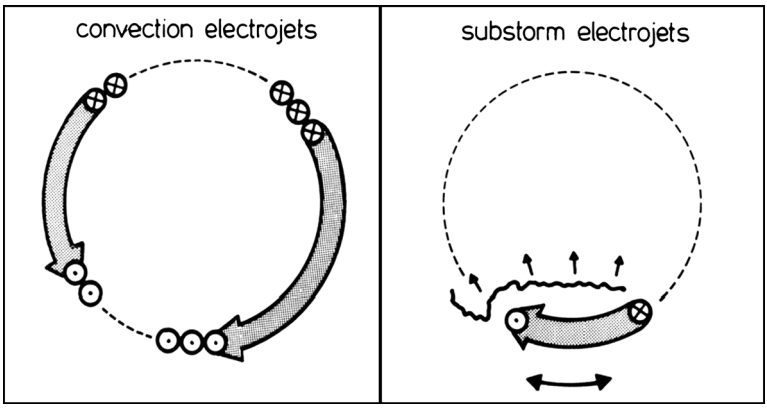

Fig. 6 Schematic diagram of location, flow direction and field-aligned current closure of the convection electrojets and the substorm current wedge (Baumjohann 1983)

B_y component. In order to emphasise the B_y effect we have selected a rather large lower limit of $|B_y|$ in the two populations: one corresponds to $B_y < -3$ nT and one to $B_y > 3$ nT.

On the day-side we clearly see the dominance of the morning and afternoon ionospheric current cell, respectively, corresponding to the sign of B_y. It is remarkable and surprising that small scale features like the cusp currents in the DPY-region are so well delineated considering the dark conditions. This must mean that sufficient particle precipitation exists in the polar cusp to create the necessary conductivity in the auroral oval and is probably related to the region 1a currents statistically found to be coincident with areas of discrete auroras (Friis-Christensen and Lassen 1991).

The availability of data from both hemispheres allows to compare the B_y effects. This confirms the known asymmetry between the B_y influence on the morning/afternoon side corresponding to the fact that merging on the day-side will split the closed near noon geomagnetic field line with one part being dragged around the Earth towards the morning side whereas the other part of the field line from the other hemisphere is being dragged towards the afternoon side, depending on the sign of B_y. We therefore see an extended afternoon cell in the northern hemisphere for $B_y > 0$ and in the southern hemisphere for $B_y < 0$.

6 IMF Effect on Observed Residuals in the Night-Side

In the night-side we notice a very strong effect in terms of enhanced positive scalar residuals on the poleward side of the electrojet near midnight. This effect corresponds to an intensified westward current in both hemispheres but in the northern hemisphere the enhancement is associated with $B_y > 3$ whereas the effect is larger in the southern hemisphere for $B_y < -3$.

As will be discussed below, the effect does not seem to be related to the plasma convection or the DP2 current system but rather to the substorm DP1 current, which is the strongest contributor to the AL index. The eastward and westward convection electrojets meet at the Harang discontinuity in the pre-midnight sector, whereas the substorm electrojet is distributed across the Harang discontinuity as sketched by Baumjohann (1983) in Fig. 6. To investigate this we plotted the B_y populations in a normal probability plot each based on two hours prior to the Harang discontinuity and two hours post midnight in Fig. 7, separately for the northern and the southern hemisphere. There is a distinct difference between the populations for positive and negative B_y but the populations are similar across the

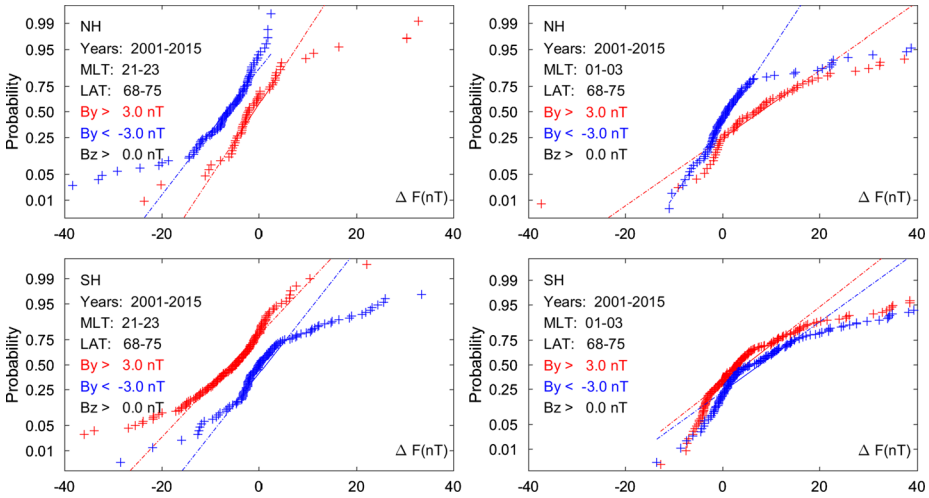

Fig. 7 Normal probability plot describing the distribution of residuals corresponding to a given magnetic local time (MLT) and latitude (LAT) interval, and for positive (*red*) and negative B_y (*blue*) respectively. Northern hemisphere (NH) (*top*) and southern hemisphere (SH) (*bottom*)

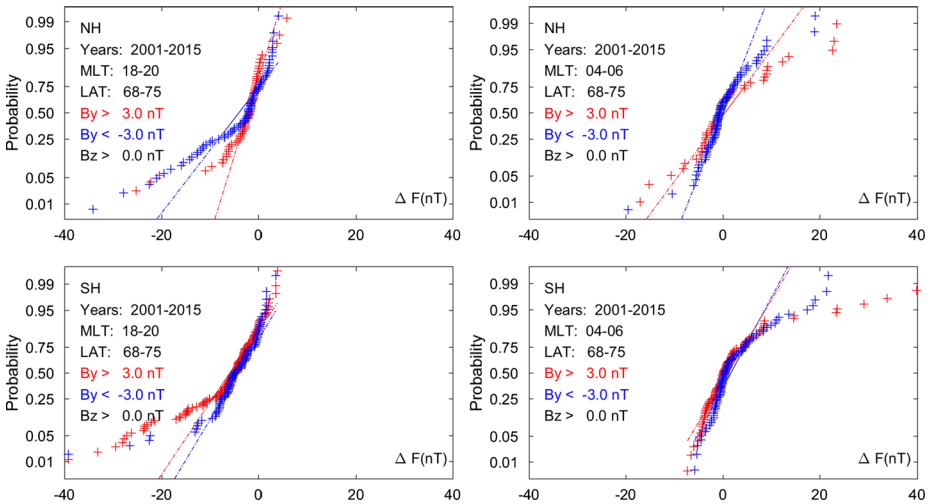

Fig. 8 Normal probability plot describing the distribution of residuals corresponding to a given magnetic local time (MLT) and latitude (LAT) interval, and for positive (*red*) and negative B_y (*blue*) respectively. Northern hemisphere (NH) (*top*) and southern hemisphere (SH) (*bottom*)

Harang discontinuity. Similar normal probability plots for periods near dawn and dusk, at magnetic local time (MLT) from 04 to 06 and from 18 to 20 in Fig. 8 show no difference in the populations for $B_y > 3$ and $B_y < -3$, except for a few very large residuals. We therefore suggest that the B_y effect is related to the substorm or the DP1 current system connected to the tail. A combination of the convection electrojet, westward in the morning and eastward in the evening, and the always westward ionospheric DP1 current, which is part of the sub-

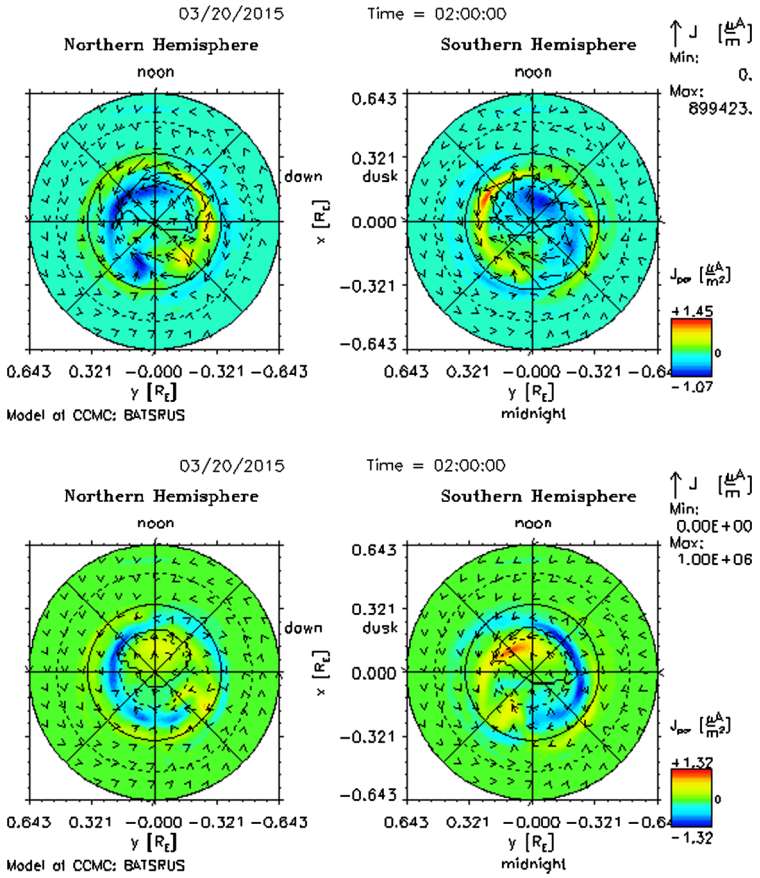

Fig. 9 Plots of ionospheric and field-aligned currents from a MHD run with corotation and also an inner magnetosphere model. The plot corresponds to 2 hours of continuous driving with solar wind $v = 500\ \mathrm{km\,s^{-1}}$, $n = 5\ \mathrm{cm^{-3}}$, $B_y = 5$ nT (*top*) and $B_y = -5$ nT (*bottom*). Both show field-aligned currents in colour and horizontal currents as vectors. Notice that in the *colour scale* positive numbers indicate currents in the direction of the magnetic field which means that in the northern hemisphere *red colours* indicate downward currents whereas the same colour in the southern hemisphere indicates upward currents

storm current wedge results in an amplification of the westward electrojet in the morning sector and a similar reduction of the eastward electrojet in the pre-midnight sector.

Kamide (1991) discusses the relationship between these two elements of the westward electrojet and concludes that the convection electrojet is driven by the plasma convection, whereas the substorm electrojet is related to an increase in the conductivity caused by enhanced precipitation. Vennerstrom et al. (2005) modelled the location and extension of the polar cap for varying B_y and B_z conditions and find that during a rotation of the B_y–B_z vector from strictly northward to eastward ($B_y > 0$) the polar cap opens up completely. During this condition upward field-aligned currents dominate the polar cap. Since the upward currents correspond to downward precipitating electrons these could provide an extra contribution to the night-side conductivity that could enhance the DP1 ionospheric current.

This interpretation seems to be consistent with MHD simulations. In Fig. 9 the resulting field-aligned and ionospheric currents after two hours of constant solar wind conditions have

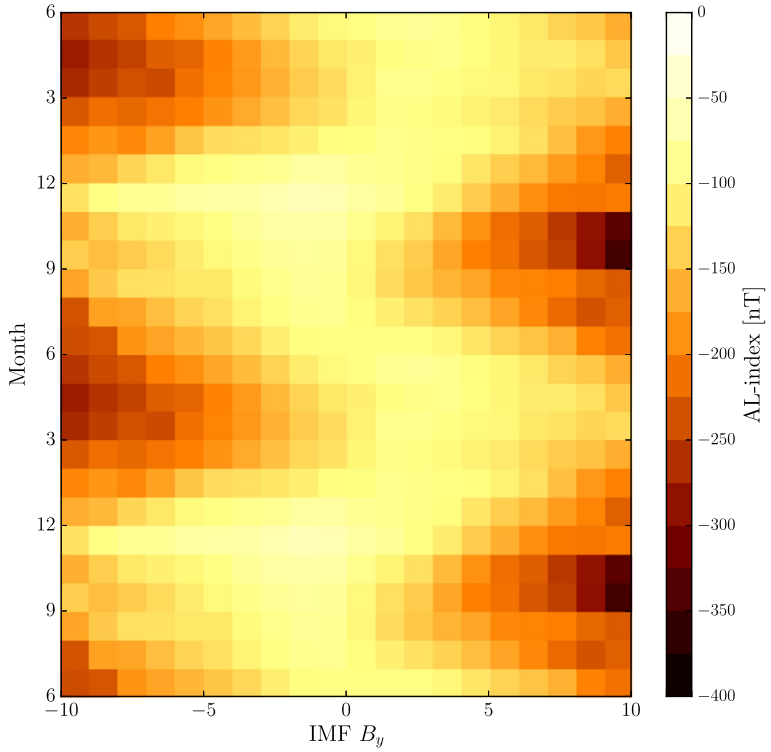

Fig. 10 Mean AL index as a function of month and IMF B_y. The figure is based on 1 min OMNI data from 1981 to 2015

been calculated based on two different IMF B_y conditions. For $B_y = 5$ nT we see a region of upward Birkeland currents in the pre-midnight sector close to the substorm region. This current region seems to be detached from the convection related afternoon upward region 1 current, which has a strong post-noon maximum. A similar effect is seen in the southern hemisphere but for $B_y = -5$ nT, also for the upward Birkeland current. This could be related to increased electron precipitation that could increase the substorm electrojet as proposed by Kamide (1991).

A corresponding B_y effect on the westward electrojet during winter was noted already by Friis-Christensen and Wilhjelm (1975) without having any explanation. That the effect is robust and not due to biased data selection is confirmed by the fact that a similar asymmetry between summer and winter is seen in the long record of the auroral electrojet index AL as demonstrated in Fig. 10.

The residual scalar magnetic field can be understood in terms of a horizontal equivalent current in the ionosphere. During sunlight this current is on average dominated by Hall currents (Laundal et al. 2015, 2016). In darkness, on the other hand it tends to be perpendicular to the Hall current in the polar cap, and antiparallel to the horizontal closure of the Birkeland current system (Laundal et al. 2015). This is consistent with the true horizontal polar cap current being close to zero. The observed B_y effect in Fig. 5, and for winter months in Fig. 10, may thus reflect a similar variation with B_y of the Birkeland currents. Indeed, Green et al. (2009) showed that the total upward and downward field-aligned currents are stronger

for positive B_y in the northern hemisphere, regardless of the sign of B_z. In the southern hemisphere, however, their results were more ambiguous.

The opposite variation with B_y in summer months in Fig. 10 may be explained in terms of a similar B_y dependence of the ionospheric convection, since Hall currents dominate in this case. Pettigrew et al. (2010) showed that the dawn convection cell, which is associated with the westward electrojet, is considerably stronger when B_y is negative during summer conditions.

7 Conclusions

We have examined the residual differences between the scalar magnetic field observed on the CHAMP and *Swarm* satellites and the CHAOS-5 main magnetic field model during the period 2000 to 2014. We find that during day-side dark winter conditions the residuals are systematically distributed consistently with the IMF dependent plasma convection systems in the polar cap and auroral oval. The result is so clear that it could lead to improved modelling of the main magnetic field or at least improved selection and a reduction in the amplitude of the residuals. We also find that night-side substorm effects are difficult to avoid in spite of careful selection of the solar wind conditions. The importance of the merging electric field is confirmed but sudden changes in the IMF orientation may also create large magnetic perturbations. A new observation is a very systematic B_y effect on the night-side residuals which we interpret as an intensification of the substorm current wedge in the northern hemisphere for $B_y > 0$ and in the southern hemisphere for $B_y < 0$.

Acknowledgements The authors are very grateful to the International Space Science Institute for inviting them to take part in the Workshop on "Earth's Magnetic Field" held in Bern in May 2015. The support of the CHAMP mission by the German Aerospace Center (DLR) and the Federal Ministry of Education and Research is gratefully acknowledged. *Swarm* L1b data were provided by ESA. For the ground magnetometer data we gratefully acknowledge: Intermagnet; USGS, Jeffrey J. Love; CARISMA, PI Ian Mann; CANMOS; The S-RAMP Database, PI K. Yumoto and Dr. K. Shiokawa; The SPIDR database; AARI, PI Oleg Troshichev; The MACCS program, PI M. Engebretson, Geomagnetism Unit of the Geological Survey of Canada; GIMA; MEASURE, UCLA IGPP and Florida Institute of Technology; SAMBA, PI Eftyhia Zesta; 210 Chain, PI K. Yumoto; SAMNET, PI Farideh Honary; The institutes who maintain the IMAGE magnetometer array, PI Eija Tanskanen; PENGUIN; AUTUMN, PI Martin Connors; DTU Space, PI Dr. Rico Behlke; South Pole and McMurdo Magnetometer, PI's Louis J. Lanzarotti and Alan T. Weatherwax; ICESTAR; RAPIDMAG; PENGUIn; British Artarctic Survey; McMac, PI Dr. Peter Chi; BGS, PI Dr. Susan Macmillan; Pushkov Institute of Terrestrial Magnetism, Ionosphere and Radio Wave Propagation (IZMIRAN); GFZ, PI Dr. Juergen Matzka; MFGI, PI B. Heilig; IGFPAS, PI J. Reda; University of L'Aquila, PI M. Vellante; SuperMAG, PI Jesper W. Gjerloev.

We thank the reviewers for valuable and constructive comments and advice.

References

W. Baumjohann, Ionospheric and field-aligned current systems in the auroral zone: a concise review. Adv. Space Res. **2**(10), 55–62 (1983)

J. Burch, P. Reiff, J. Menietti, R. Heelis, W. Hanson, S. Shawhan, E. Shelley, M. Sugiura, D. Weimer, J. Winningham, IMF B_y-dependent plasma flow and Birkeland currents in the dayside magnetosphere: 1. Dynamics Explorer observations. J. Geophys. Res. Space Phys. **90**(A2), 1577–1593 (1985)

S. Cowley, M. Lockwood, Excitation and decay of solar wind-driven flows in the magnetosphere-ionophere system, in *Annales Geophysicae*, vol. 10, 1992, pp. 103–115, Copernicus

N. Crooker, Dayside merging and cusp geometry. J. Geophys. Res. Space Phys. **84**(A3), 951–959 (1979)

J.W. Dungey, Interplanetary magnetic field and the auroral zones. Phys. Rev. Lett. **6**(2), 47 (1961)

C.C. Finlay, N. Olsen, L. Tøffner-Clausen, DTU candidate field models for IGRF-12 and the CHAOS-5 geomagnetic field model. Earth Planets Space **67**(1), 114 (2015)
C.C. Finlay, V. Lesur, E. Thebault, F. Vervelidou, A. Morschhauser, R. Shore, Challenges handling magnetospheric and ionospheric signals in internal geomagnetic field modelling. Space Sci. Rev. (2016, this issue). doi:10.1007/s11214-016-0285-9
E. Friis-Christensen, K. Lassen, Large-scale distribution of discrete auroras and field-aligned currents, in *Auroral Physics*, vol. 1, 1991, pp. 369–381
E. Friis-Christensen, H. Lühr, G. Hulot, *Swarm*: a constellation to study the Earth's magnetic field. Earth Planets Space **58**, 351–358 (2006)
E. Friis-Christensen, J. Wilhjelm, Polar cap currents for different directions of the interplanetary magnetic field in the $Y-Z$-plane. J. Geophys. Res. **80**, 1248–1260 (1975)
E. Friis-Christensen, K. Lassen, J. Wilhjelm, J.M. Wilcox, W. Gonzales, D.S. Colburn, Critical component of the interplanetary magnetic field responsible for large geomagnetic effects in the polar cap. J. Geophys. Res. **77**, 3371–3376 (1972)
E. Friis-Christensen, Y. Kamide, A.D. Richmond, S. Matsushita, Interplanetary magnetic field control of high-latitude electric fields and currents determined from Greenland magnetometer data. J. Geophys. Res. **90**, 1325–1338 (1985)
N. Fukushima, Generalized theorem for no ground magnetic effect of vertical currents connected with Pedersen currents in the uniform-conductivity ionosphere. Rep. Ionos. Space Res. Jpn. **30**(1–2), 35–40 (1976)
J. Gjerloev, A global ground-based magnetometer initiative. Eos **90**(27), 230–231 (2009)
J. Gjerloev, The SuperMAG data processing technique. J. Geophys. Res. Space Phys. **117**(A9) (2012)
D.L. Green, C.L. Waters, B.J. Anderson, H. Korth, Seasonal and interplanetary magnetic field dependence of the field-aligned currents for both Northern and Southern Hemispheres. Ann. Geophys. **27**, 1701–1715 (2009). doi:10.5194/angeo-27-1701-2009
T. Iijima, T. Potemra, L. Zanetti, P. Bythrow, Large-scale Birkeland currents in the dayside polar region during strongly northward IMF: a new Birkeland current system. J. Geophys. Res. Space Phys. **89**(A9), 7441–7452 (1984)
Y. Kamide, The auroral electrojets: relative importance of ionospheric conductivities and electric fields, in *Auroral Physics*, vol. 1, 1991, p. 385
J. Kan, L. Lee, Energy coupling function and solar wind-magnetosphere dynamo. Geophys. Res. Lett. **6**(7), 577–580 (1979)
K. Kauristie, A. Morschhauser, N. Olsen, C.C. Finlay, R.L. McPherron, J.W. Gjerloev, H.J. Opgenoorth, On the usage of geomagnetic indices for data selection in internal field modelling. Space Sci. Rev. (2016, this issue). doi:10.1007/s11214-016-0301-0
L. Kother, M.D. Hammer, C.C. Finlay, N. Olsen, An equivalent source method for modelling the global lithospheric magnetic field. Geophys. J. Int. **203**, 553–566 (2015)
K.M. Laundal, S.E. Haaland, N. Lehtinen, J.W. Gjerloev, N. Ostgaard, P. Tenfjord, J.P. Reistad, K. Snekvik, S.E. Milan, S. Ohtani, B.J. Anderson, Birkeland current effects on high-latitude ground magnetic field perturbations. Geophys. Res. Lett. **42**(18), 7248–7254 (2015)
K.M. Laundal, J.W. Gjerloev, N. Ostgaard, J.P. Reistad, S.E. Haaland, K. Snekvik, P. Tenfjord, S. Ohtani, S.E. Milan, The impact of sunlight on high-latitude equivalent currents. J. Geophys. Res. (2016). doi:10.1002/2015JA022236
S. Milan, Modeling Birkeland currents in the expanding/contracting polar cap paradigm. J. Geophys. Res. Space Phys. **118**(9), 5532–5542 (2013)
P.T. Newell, T. Sotirelis, K. Liou, C.-I. Meng, F.J. Rich, A nearly universal solar wind-magnetosphere coupling function inferred from 10 magnetospheric state variables. J. Geophys. Res. **112**(A1) (2007). doi:10.1029/2006JA012015
A. Nishida, K. Maezawa, Two basic modes of interaction between the solar wind and the magnetosphere. J. Geophys. Res. **76**(10), 2254–2264 (1971)
N. Olsen, H. Lühr, T.J. Sabaka, M. Mandea, M. Rother, L. Tøffner-Clausen, S. Choi, CHAOS – a model of Earth's magnetic field derived from CHAMP, Ørsted, and SAC-C magnetic satellite data. Geophys. J. Int. **166**, 67–75 (2006)
N. Olsen, H. Lühr, C.C. Finlay, L. Tøffner-Clausen, The CHAOS-4 geomagnetic field model. Geophys. J. Int. **1997**, 815–827 (2014)
E.D. Pettigrew, S.G. Shepherd, J.M. Ruohoniemi, Climatological patterns of high-latitude convection in the Northern and Southern hemispheres: dipole tilt dependencies and interhemispheric comparison. J. Geophys. Res. **115** (2010). doi:10.1029/2009JA014956
P.H. Reiff, J. Burch, IMF B_y-dependent plasma flow and Birkeland currents in the dayside magnetosphere: 2. A global model for northward and southward IMF. J. Geophys. Res. Space Phys. **90**(A2), 1595–1609 (1985)

A. Ridley, G. Lu, C. Clauer, V. Papitashvili, A statistical study of the ionospheric convection response to changing interplanetary magnetic field conditions using the assimilative mapping of ionospheric electrodynamics technique. J. Geophys. Res. Space Phys. **103**(A3), 4023–4039 (1998)

P. Ritter, H. Lühr, S. Maus, A. Viljanen, High latitude ionospheric currents during very quiet times: their characteristics and predictabilities. Ann. Geophys. **22**, 2001–2014 (2004)

S. Vennerstrom, T. Moretto, L. Rastätter, J. Raeder, Field-aligned currents during northward interplanetary magnetic field: Morphology and causes. J. Geophys. Res. Space Phys. **110**(A6) (2005)

J. Wilhjelm, E. Friis-Christensen, T.A. Potemra, The relationship between ionospheric and field-aligned currents in the dayside cusp. J. Geophys. Res. **83**, 5586–5594 (1978)